JOURNAL OF MATERIALS SCIENCE **35** (2000) 3785–3792

Evaluation of damping and elastic properties of composites and composite structures by the resonance technique

C. Y. WEI*, S. N. KUKUREKA
The University of Birmingham, School of Metallurgy and Materials, Edgbaston, Birmingham, B15 2TT, UK
E-mail: S.N.kukureka@Bham.ac.uk

This paper describes the resonance technique for determining the stiffness and damping properties of a composite or composite structure. Pultruded GRP composites and optical fibre cables (multi-component structures) were investigated. The resonance frequencies (natural frequencies) of a material, or a system, are a function of its elastic properties, dimensions and mass. This concept is used to determine the stiffness of a vibrated material by the resonance technique, which applies only very low stresses through the application of acoustic energy. This makes it applicable to measure the stiffness of multi-element cables. The damping properties, in terms of Q^{-1} (internal friction) were determined by both a free exponential decay curve and half-peak bandwidth methods. The influence of specimen length and measurement set-up was investigated. The applicability and accuracy of the resonance technique for a composite structure were discussed. The measured elasticity of optical cables was found to be in good agreement with the derived theoretical value.

1. Introduction

The dynamic resonance technique has been used to evaluate the modulus and damping behaviour of a variety of materials, including metals [1, 2], ceramics [3], polymers [2], metal matrix composites [4, 5] and, in a limited way, polymer-matrix composites [6–8]. The few tests on composites have been on graphite/epoxy or hybrid laminates. This method has also found some use in particular 'composite structures'. For instance, Nishino [9] evaluated the amplitude dependence of internal friction in thin films on substrates. Wang [10] investigated the damping properties of an acrylic-cored, laminated steel using cantilever-beam specimens. However there have not been any reports of its application to either GRP pultruded rods, or to high-damping, multi-element structures such as cables. It is the aim of this project to evaluate the technique for these applications.

The longitudinal modulus is determined by exciting one end of a specimen and picking up the response at the other end [11]. Torsional elasticity can be measured by applying a sinusoidal wave in a torsional manner [12]. Flexural resonance measurements can be made in two ways: cantilever vibration [4] and free-free vibration [13]. The free-free vibration mode is the method used in this project to evaluate stiffness and damping behaviour.

Aerial cables experience static and dynamic stresses. Dynamic movements cause a complex damage history which is harder to quantify than is static load damage. High damping structures and high damping materials can effectively attenuate vibration. Ideal cable structures possess a high damping capacity, in combination with flexibility for easy handling, and with high stiffness in the longitudinal direction. Damping behaviour is a basic concept in dynamic analysis. The damping factor is a material parameter reflecting the capacity for energy absorption. The energy absorption in elastic materials, such as metals, and ceramics, is generally due to defects and cracks. For polymer materials, damping is mostly caused by viscoelasticity (the strain response lagging behind the applied stresses). In fibre-reinforced composites, interfaces between fibres and the matrix play a major role in damping. For polymer materials, DMTA (dynamic mechanical thermal analysis) is widely used to obtain the loss factor, which is linked with damping properties. However, this method is not sensitive enough to obtain the loss factor of a fibre composite which is much stiffer than a polymer.

A telecommunications cable is comprised of many elements which are only held together by the outer sheath. In all dielectric self-supporting (ADSS) optical cables, pultruded GRP rods and aramid-fibre yarns are widely used as a load-bearing elements, or strength members. These materials are immune to electromagnetic interference and radio frequency interference

* Now at Cranfield University, School of Industrial and Manufacturing Science, Cranfield, Bedfordshire, MK43 0AL.

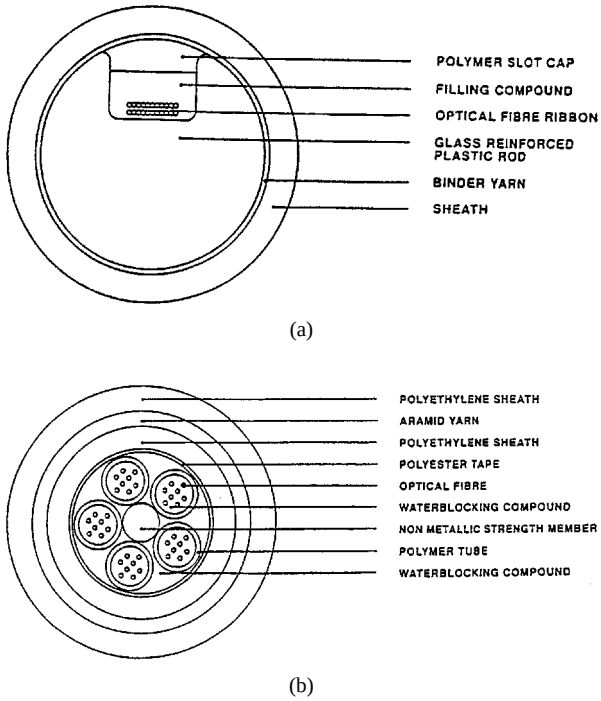

Figure 1 (a) Cable A: optical cable structure with a slotted GRP rod as strength member. (b) Cable B: optical cables with a central GRP rod and peripheral laid aramid fibre yarns as strength members.

when the cables are suspended next to high-voltage power lines. Fig. 1a and b show the structure of the cables in which GRP rods and aramid fibres are used as strength members. Conventional mechanical bending tests are not applicable to determine the stiffness of these cable structures because sliding between elements will occur when mechanical stresses are applied. In resonance measurements, the specimens are excited by acoustic energy. Sliding between elements of cables, produced by this very small stress, can be taken to be negligible. Once the resonance frequencies of a cable are obtained, the stiffness and damping properties can be determined.

2. Materials and resonance measurements

2.1. Materials

Two types of all dielectric self-supporting (ADSS) cables were evaluated with the structures shown in Fig. 1a and b, (both of which were manufactured by Pirelli Cables Ltd.) Cable A contains a single 10 mm slotted GRP rod as a strength member. In Cable B, a layer of aramid fibre yarns as the principal strength member is peripherally wrapped around the inner polymer sheath which accommodates the optical fibres. Two types of polymer sheath were examined with Cable B. One is medium density polyethylene (MDPE) and the other one is a copolymer of ethylene-vinyl acetate (EVA). The GRP strength members, which were investigated, are pultruded 3.0 mm circular rods and 10.0 mm slotted rods. The structure of the latter type is illustrated in Fig. 2. Both strength members are E-glass/epoxy unidirectional composites. The circular rods contain 70% of glass fibres by volume while the fibre volume fraction of the slotted rods is 65%.

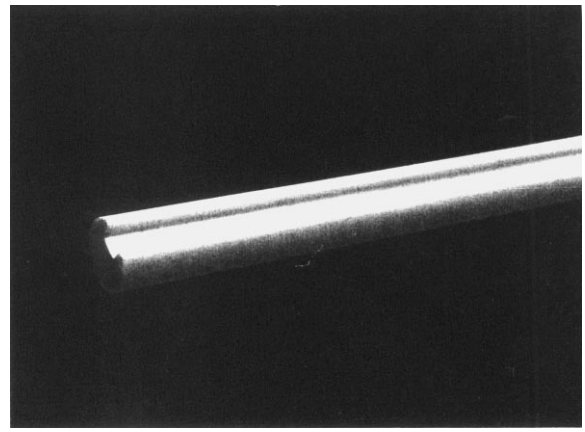

Figure 2 Configuration of a slotted GRP pultruded rod.

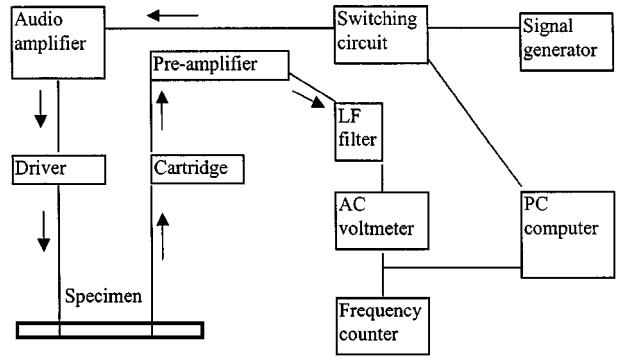

Figure 3 Schematic diagram of the dynamic resonance measurement.

2.2. Measurement technique

The device used in measuring resonant frequencies, is illustrated in Fig. 3. The main function of the components is to excite and detect resonant frequencies. The device can apply waveforms in a wide range of frequencies from an audio oscillator. As the oscillator frequency is scanned, it eventually reaches one of the mechanical resonance frequencies of the specimen. The amplitude of the output signals will show a tremendous increase at the system resonant frequencies. This increased amplitude is detected by the pickup, in contact with the specimen. The spectrum of amplitude response to frequency can be recorded through a computer and analysed using a fast fourier transform (FFT).

The system locates the oscillating system resonance, and exhibits the relative magnitude of the resonance peaks. From the magnitude of the peaks, it is possible to define the fundamental, second and third resonance. The fundamental resonance is the largest peak, and it can easily be detected. Thus only the fundamental resonance was used to calculate stiffness and damping.

2.3. Specimen suspension

There are many ways for coupling the energy from the driver to specimens and detecting these vibrations [14]. For instance, the specimens may rest on foam rubber at the nodal points, or on a thick foam rubber pad in which the vibration is transmitted directly through a rod to an appropriate part of the massive specimens. The suspension method used here is two cotton threads, one

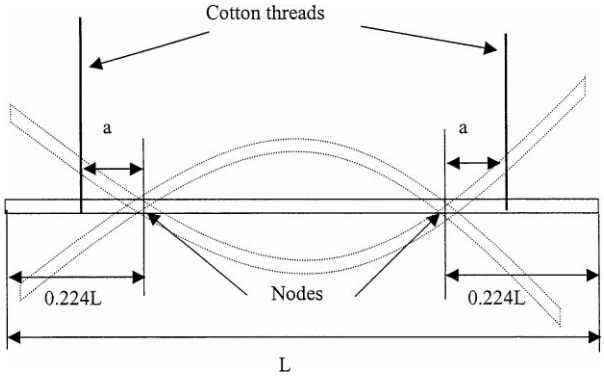

Figure 4 Specimen motion in the flexural fundamental vibration mode and the suspension arrangement of cotton threads.

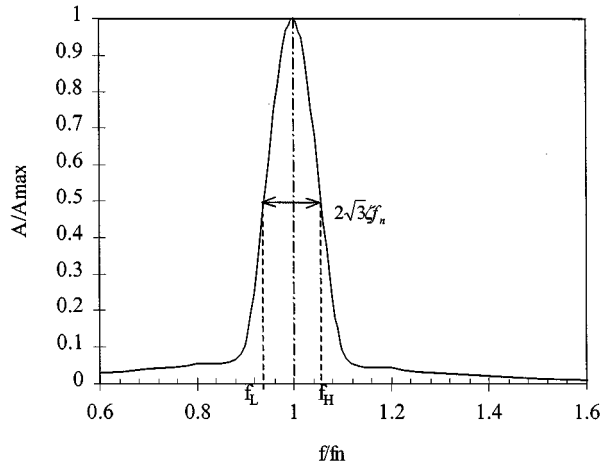

Figure 5 Diagram illustrating the definition of Q^{-1} from a resonant peak.

being attached to a driver and the other being attached to a stylus as a pickup as shown in Fig. 3. In respect of the fundamental flexural resonance mode, the motion of different parts of a specimen is illustrated in Fig. 4, showing in-phase oscillation at the two ends, out of phase oscillation in the centre part, and no motion at the two nodal points. In this mode, the two nodal points are located at $0.224L$ away from the two ends where L is the length of a specimen. There is no motion at nodal points, which are $0.224L$ away from the two ends in the fundamental flexural resonance. These two points were marked on the specimens before the test, because the two suspension lines should be located the same distance away from the nodes as in Fig. 4. Although the suspension position can be either outside or inside the node position, most measurements were conducted when the threads were located 6 mm outside the nodes. This is because the test specimen was steadily suspended, and the response amplitude could easily be detected. In order to determine the influence of the suspension positions on the measured results, the cotton threads were always positioned at the same distance, (a or $-a$), away from the nodes.

The length of specimens depends on their diameters and weights. Basically, thinner specimens were cut to have a shorter length, and vice versa. In principle, a relatively higher ratio of span to thickness produces a larger output in amplitudes at the same input power. Typical lengths and weights for the 3.0 GRP rods were around 110 mm, and 1.57 g respectively, whereas those for the slotted GRP rods were about 180 mm and 24 g. Specimens were weighed to ± 0.001 g, and the diameters were measured to ± 0.02 mm.

Cable A is mainly comprised of a slotted GRP rod and a polymer sheath. Compared with Cable B which contains aramid fibres as strength members, Cable A is rather stiffer and was cut to 180 mm long for the measurements. Cable B as shown in Fig. 1b, consists of a MDPE (medium density polyethylene) sheath, and was cut to be 214 mm long for the measurement.

3. Evaluation of damping and stiffness via resonance

3.1. Evaluation of the damping level of a vibrated system

Damping is associated with the dissipation of energy in a vibrated system. The diminution of the vibration amplitude with time is evidence of the effect of damping. One common way to quantify damping in a system is to measure the rate of decay of a free oscillation. A free vibration can be produced in a system by suddenly removing an applied oscillating force. The peak amplitudes follow an exponential decay given by:

$$A = A_0 e^{-2\pi\zeta f_n t} \tag{1}$$

where: A is the amplitude at time t; A_0 is the amplitude when the oscillating force is removed, f_n is the system natural frequency. ζ is damping ratio, which determines the system damping capacity. A quantity, Q^{-1}, known as the internal friction of a material, can be obtained from the damping ratio by:

$$Q^{-1} = 2\zeta \tag{2}$$

The internal friction is a measure of the breadth of the resonance peak. The value is also given by:

$$Q^{-1} = \frac{f_h - f_l}{\sqrt{3} f_n} \tag{3}$$

where, f_h, and f_l are frequencies above and below the natural frequency at an amplitude of half the maximum resonant amplitude. This method is called the half-peak bandwidth method.

Fig. 5 shows the physical significance of Equation 3 in defining Q^{-1} by the frequencies at half the peak of the resonant amplitude. The bandwidth of a resonant peak is determined by the internal friction and the natural frequency of an oscillating system. A particular system has its specific natural frequencies. Thus the bandwidth is a function of the internal friction.

3.2. The calculation of modulus from resonant frequencies

The equations for calculating the modulus of elasticity were first developed by Pickett [15]. The relationship between modulus of elasticity and resonance frequencies is determined by means of the formula:

$$E = CWf^2 \tag{4}$$

where: W = weight of the specimen, f = resonant frequency, C = a factor which depends on the dimensions of the specimen, the mode of vibration and Poisson's ratio.

To obtain E, C must be determined. The expression for C can be written as:

$$C = \frac{4\pi^2 l^2}{g m^4 I} T \tag{5}$$

where: g = the acceleration due to gravity, l = the length of specimen, and, I = the second moment of area of the cross-section. m, is a factor, the value of which depends on the mode of vibration. For the first mode of vibration, $m_1 = 4.73$.

T is a correction factor introduced by Goens [16] and based upon the accurate differential equations giving the relationship between the resonant frequencies and the modulus. Spinner and Tefft [14] modified T to the expression:

$$T = 1 + 6.585(1 + 0.0752\mu + 0.8109\mu^2) \times \left(\frac{d}{l}\right)^2 - 0.868\left(\frac{d}{l}\right)^4 - \frac{8.34(1 + 0.2023\mu + 2.173\mu^2)\left(\frac{d}{l}\right)^4}{1 + 6.338(1 + 0.14081\mu + 1.536\mu^2)\left(\frac{d}{l}\right)^2} \tag{6}$$

where: μ is Poisson's ratio (for fibre composites, $\mu = 0.27$), d/l is the ratio of the diameter to the length of specimens.

For 10 mm slotted GRP rods in the fundamental mode of vibration, when $d/l = 0.05$, the correction factor can be obtained from Equation 6 as $T_1 = 1.018495$. Then, once the fundamental resonant frequency is detected, the modulus of elasticity for the slotted GRP rods can be calculated by combining Equations 4 and 5

$$E = \frac{0.078791 l^2 w f_1^2 T_1}{I} \tag{7}$$

When specimens have a circular cross-section, the equation for calculating the elastic modulus is written as:

$$E = 1.261886 \frac{\rho l^4}{d^2} f_1^2 T_1 \tag{8}$$

where f_1 is the first resonant frequency.

4. Results and discussion

From the resonance measurements, the following parameters were determined: resonant frequencies, response spectra of amplitude to frequencies, half-peak bandwidth frequencies. The stiffness and damping (internal friction) could be calculated from the measured frequencies.

4.1. Response spectra of amplitude with frequency

When input signals with a wide range of frequencies, (from 0 to 12 kHz), were applied to the specimens, a spectrum of amplitude response to this range of frequencies is recorded in a PC computer. Spectra of 3.0 mm GRP rods, and 10.0 mm slotted GRP rods are shown in Figs 6 and 7. Two peaks from the smaller rods were observed in Fig. 6 within a frequency range from 0 to 5000 Hz. The peak with the higher resonance amplitude is located at 1100 Hz. The second peak with much lower amplitude appears at 3280 Hz, which is the second resonance. Both the resonant frequencies can be used to calculate the value of stiffness by selecting m appropriately in Equation 5, which gives the result as 50.8 GPa. The slotted GRP rods show the first three resonant peaks at 1220 Hz, 3090 Hz and 4400 Hz, respectively, as shown in Fig. 7. In forced vibration, the first and second peaks are responsible for 90% of the strain amplitude [17]. The amplitude of the fundamental resonance is much larger than that of the second. For the 3.0 mm rods, the third resonance peak seems too weak to be detected by this device. In previous research and applications of damping behaviour, more emphasis has been put on the first, rather than the second or higher resonance peaks.

Cables exhibit much high damping behaviour than GRP rods because they contain a polymer sheath (such as PE or EVA), which is a typical viscoelastic material. Particularly in Cable B with aramid fibres as strength members, much interface friction occurs during vibration as elements inside the cable are only loosely bonded together. Consequently, these materials give wide resonance peaks with low amplitudes. In Fig. 8,

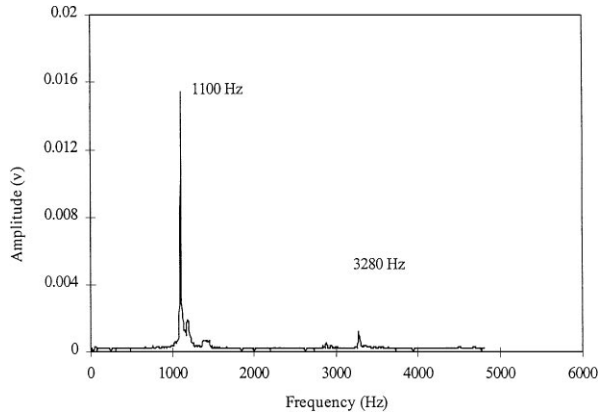

Figure 6 Response of amplitude to frequencies in the 3.0 mm GRP rods.

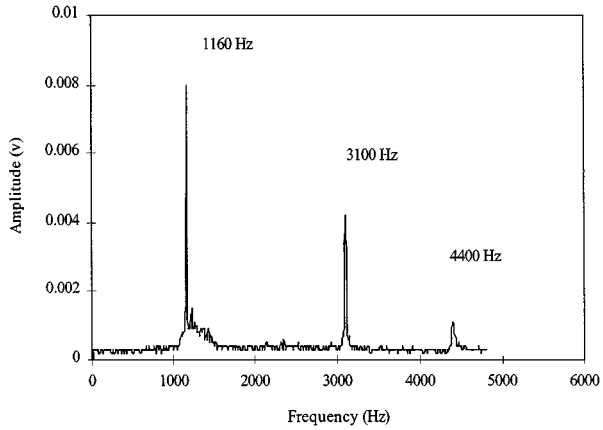

Figure 7 Response of amplitude to frequencies in the 10.0 mm slotted GRP rods.

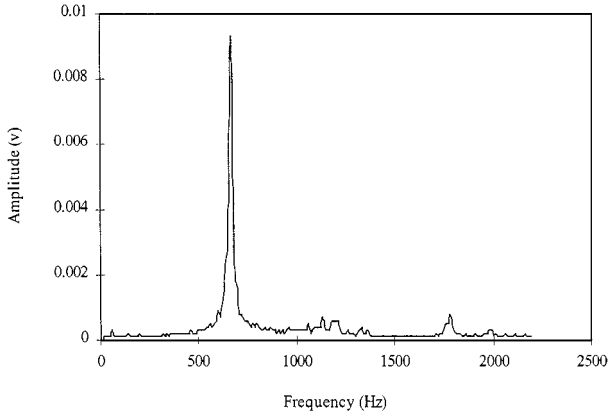

Figure 8 Spectrum of amplitude response to frequencies in Cable A.

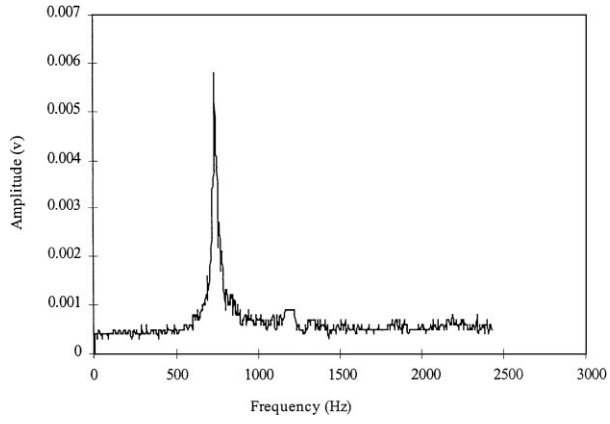

Figure 9 Spectrum of amplitude response to frequencies in Cable B with PE sheath.

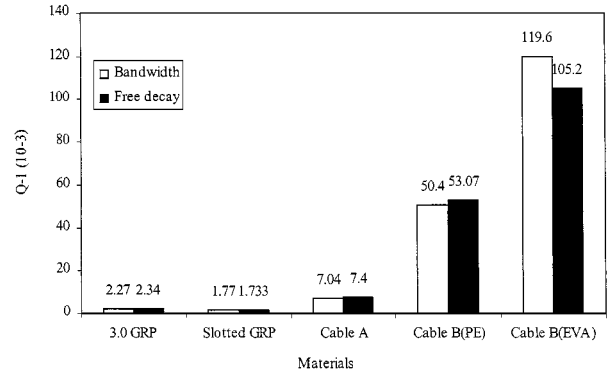

Figure 10 Damping value obtained from half peak bandwidth and free decay (logarithmic decrement).

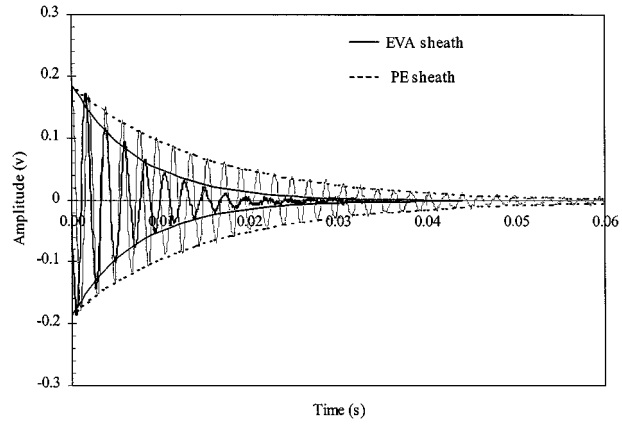

Figure 11 Logarithmic decrement of free decay vibration in Cable B showing higher damping with EVA sheath and lower damping with PE sheath.

the plot of amplitude response to frequencies in Cable A shows a sharp first resonant peak at 670 Hz, and a small second resonant peak at 1790 Hz. However, in the spectra of Cable B (as shown in Fig. 9), only the first peak can be seen. The output signals of the second peak are too weak to be detected, as such weak signals can be swamped by device electrical signals.

4.2. Damping measured by the free decay curve and half-peak bandwidth

As described in Equations 1 and 3, the damping factor can be obtained from either the exponential free decay curve [3] or the bandwidth at the resonance peak [1, 2]. The results of damping measured by the above two methods were compared in Fig. 10 which shows the damping values of five types of material or structure. In general, these two methods give a very similar result for each material or structure. However, for a high damping material, the deviation tends to become larger. The deviation of the damping value obtained from the two methods reaches 12% in Cable B with a EVA sheath, whose damping factor is over 0.1. For the rest of materials whose damping value is much lower, the deviations are within 6.0%. In free vibration of the GRP materials, the amplitude of vibration is attenuated, reaching zero after a large number of cycles. However, it takes only a few cycles for the amplitude to approach zero when free vibration occurs in a high damping structure (Cable B). Fig. 11 shows the trace of amplitudes when Cable B with MDPE and EVA sheaths was subjected to free vibration. In the plots, the exponential equation (Equation 1) was used to fit the decay of amplitude. A good fit is obtained indicating that the logarithmic decrement is applicable to evaluate the damping values. The high deviation which occurred in high damping materials is believed to result from the error in fitting the exponential equation because only a small number of cycles were available (Cable B with EVA sheath). In the high damping system, the band-width method, in comparison, becomes a more accurate method of determining the damping factor. Also the measurement by bandwidth is easier and simpler. Therefore the damping data in this paper were obtained via the half-peak bandwidth route.

4.3. Stiffness and damping factor of materials

The measured values of stiffness and internal friction of GRP materials and optical cables are summarised in Table I, in which the modulus of the GRP materials predicted by the rule of mixtures is also listed. The elastic properties of unidirectional composites are determined by the elastic properties of the constituents and their volume fractions, when a tensile or compressive load is applied to fibres. This is known as the rule of mixtures. In terms of unidirectional composites, the

TABLE I Flexural modulus and internal friction of GRP rods

Materials	Modulus (GPa)	Standard deviation (GPa)	Theoretical modulus (GPa)	Q^{-1} (10^{-3})	Standard deviation (10^{-3})
3.0 mm circular GRP	52.43	0.6	51.4	2.48	0.24
10.0 mm slotted GRP	45.66	0.56	47.8	1.75	0.04
Cable A	12.05	0.05	10.5	0.72	0.02
Cable B (MDPE)	4.34	0.08	N/A	41.56	0.17

rule of mixtures can be appropriately applied when the materials are subjected to a flexural load, as fibres are evenly distributed in the matrix. E-glass fibres have a modulus of 72.4 GPa, while the modulus of epoxy resin is only 2.45 GPa [18]. The modulus of GRP rods was calculated and listed in Table I based on the measured fibre volume fraction. The modulus values measured by the resonant technique are very close to the calculated values for circular and slotted GRP rods. The measured value for the circular GRP is slightly higher than the value predicted. In the resonance measurement, only a micro-scale stress was applied to the materials via acoustic waves. The modulus used to calculate the value has been measured mechanically by an applied large stress. An imperfect elastic material shows a higher modulus when a lower stress is applied. However, the slotted GRP shows a slightly lower value than the predicted value. This result is probably caused by the calculation error in the second moment of area of the slotted cross-section rod. In the calculation, a geometrical simplification has been made, which leads to an over-estimated value of I in Equation 5, which results in a slightly lower modulus. However the standard deviation coefficient in a set of five tests is only around 1.0%, which shows that the measurement is very consistent.

The accuracy of the stiffness is determined by the accurate measurements of specimen dimensions, weight, and the resonant frequency, as seen in Equations 7 and 8. The apparatus was experimentally able to measure natural frequencies accurately to ± 0.5 Hz. This deviation will only create an error of 0.02% in a stiffness of 4 GPa in Cable B (MDPE).

4.4. Theoretical values of stiffness of cables

To validate the measured stiffness of the cables obtained by the resonance technique, it is possible to derive the theoretical value from the structure and component elasticity. The term, 'stiffness', is adopted here to describe the relationship of stress to deflection, rather than flexural modulus. Stiffness prediction in the structure of Cable B is much more complex, as the contribution from aramid yarns is unknown, although it is possible to predict the tensile modulus of the cables provided that the quantity and modulus of individual elements is known. To predict the stiffness of Cable A is practicable, as the stiffness is mainly determined by the outside PE sheath, and the core-slotted GRP rods. Also, the amounts and stiffnesses of these two materials are known. A presumption must be made that there is no sliding between the sheath and core rods under the stress transverse to the longitudinal direction. This presumption is realistic in the application of the dynamical resonance measurements because of the very negligible stress applied, which is unlikely to cause sliding.

Flexural rigidity is defined as EI (the value of flexural modulus multiplied by second moment of area). The stiffness of a multi-layer structure is related to the stiffness of individual layers by:

$$EI = E_1 I_1 + E_2 I_2 + \cdots + E_n I_n \tag{9}$$

where subscripts $1, 2, \ldots n$, stand for constituents of a material or structure.

In order to simplify the calculation, only two constituents (PE sheath and the GRP core) are considered to comprise Cable B. Here subscript 1 represents the PE sheath, and 2 represents the core GRP rods.

I_1 is the second moment of area of the PE sheath, given by:

$$I_1 = \frac{1}{8}\pi d_1^3 t \tag{10}$$

where d_1 is the diameter of centre line of the PE sheath; t is the thickness of the sheath; I and I_2 are the second moment of area of the whole cable and the core rod, respectively. I_2 has been calculated to have a value of 320.1 mm^4 [19].

Thus, the stiffness of the whole cable can be obtained from:

$$E = \frac{E_1 I_1 + E_2 I_2}{I} \tag{11}$$

When, $E_1 = 0.2$ GPa (measured by DMTA), and $E_2 = 47.16$ GPa (from Table I). The theoretical value of E for Cable A calculated by Equation 11 as 10.6 GPa.

Compared with the stiffness determined from the resonant frequency ($E_{\text{exp}} = 12.05$ GPa in Table 1), the measured value is 12% higher than the theoretical value. When calculating the stiffness, the contribution from the other elements, such as the slot cap and binder yarns as shown in Fig. 1a was neglected to simplify the calculation. This makes the predicted value lower than the measured value. Consequently, we have reason to believe that the measured value is closer to the real value.

4.5. The influence of suspension positions and specimen length

As described previously, the resonance measurement was conducted using two cotton threads to suspend specimens. It is necessary to examine the influence of the suspension position on measured values. Also this examination was carried out using different length of specimens to examine the influence on the results when the suspension position remained unchanged. The

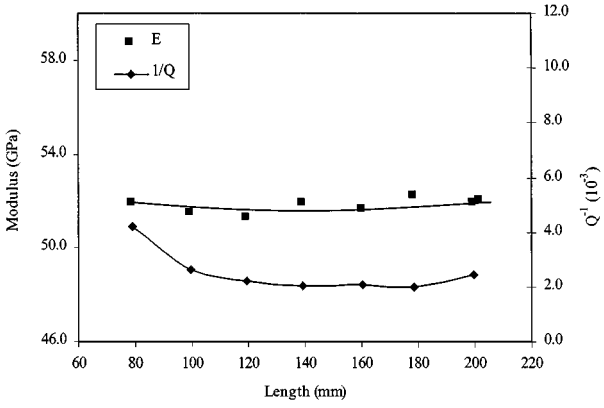

Figure 12 Modulus and damping factor vs. specimen lengths in the 3.0 mm GRP rods.

examination was performed on 3.0 mm GRP rods with lengths ranging from 80–200 mm. The results are plotted in Fig. 12 showing the variation of stiffness and damping ratio with specimen length. As shown in Fig. 4, no amplitude results when the cotton threads are placed at the two nodes in the fundamental vibration mode. The specimen should, therefore, be suspended at positions away from the nodal points. This investigation was continued by changing the suspension positions–with both at the same distance away from the nodes. The results for E and Q^{-1} are plotted against suspension position in Fig. 13.

As shown in Fig. 12, the measured values vary within the range 51.27–52.25 GPa (ie almost constant) when different specimen lengths are used. Such a small variation could be from the natural scatter of material properties. The results suggest that specimen length has no significant effect on the measured value of stiffness. Fig. 12 also shows that damping in the GRP rods is not affected by the specimen length, except that the shortest specimen appears to exhibit higher damping. A coupling effect (or interference) between the test system and specimen may easily occur when a light specimen is oscillated. For instance the shortest rod weighs only 0.85 g. Also the output signals are not stable enough to determine an accurate resonance peak if specimens have a very large ratio of length to diameter. For example, when the length exceeds 200 mm for the GRP rods with a diameter of 3.0 mm, it is unlikely that a stable response will be achieved.

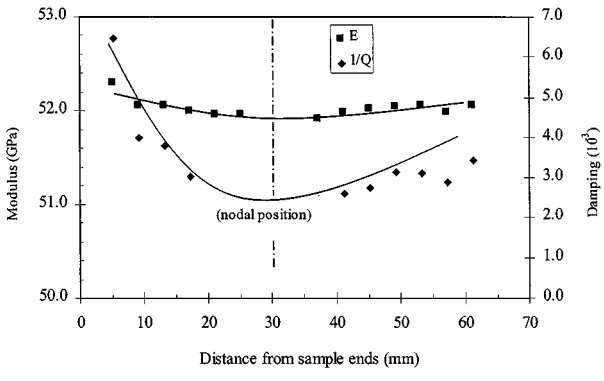

Figure 13 Variation in modulus and damping factor with suspension positions in the 3.0 mm GRP rod with a length of 140 mm.

Fig. 4 displays the response of amplitude in different parts of a rod in the fundamental flexural mode. The magnitude of the amplitude is clearly a function of the distance to the nodes. How the suspension position affects the measured values in stiffness and damping can be perceived from Fig. 13. It is interesting to note that the relationship of internal friction to suspension position has a very similar trend to that reflected by the amplitude curve (in Fig. 4). The damping values are at a minimum when the suspension positions are close to the nodes. The variation in stiffness shows a similar trend (the lowest value is around the nodes), but the suspension position has a smaller effect on the stiffness values than on the damping values. The rapid decay of vibration, which occurs at a higher amplitude, may be interpreted as the larger damping when specimens are suspended either close to the ends or close to the middle of the specimens. The suspension position recommended is close to the nodes in order to achieve a good result [14].

5. Conclusions

The resonance technique was employed to evaluate the stiffness and damping properties of GRP composites and optical cables. A free-free flexural vibration mode was applied to obtain the flexural modulus and internal friction values. This technique produces accurate values of modulus and damping for stiff materials (i.e. composites) and high damping, multi-element, composite structures (i.e. optical cables). The damping value can be obtained from either the exponential free decay curve or the half-peak bandwidth. For high damping structures, the latter approach is recommended to obtain a more accurate value. The stiffness of a simple cable structure has been predicted from the behaviour of its constituents. The predicted values have shown that the technique can evaluate the real properties of the structures. The position where specimens are suspended affects the values of the damping value, but has little effect on the values of stiffness. The specimen dimensions have no influence on the measured stiffness and damping values within a large range. However, a proper range of weight and dimension has to be selected to achieve a good resonance response according to the instrumental capability and depending on the materials. In conclusion, the resonant technique appears a reliable and consistent method for evaluating the dynamic behaviour of composites and high-damping, multi-element structures.

Acknowledgements

Acknowledgements to Pirelli Cables Ltd which supplied all the test materials and partly sponsored this work. Particular thanks go to Mr Martin Davies, Mr Ralph Sutehall and Mr Ian Lang for their help and collaboration. The authors would like to thank Dr David Pearce, Dr Lee Tims and Dr Clive Ponton for help with the resonance measurements and valuable discussions. The help of the Royal Society and the School of Metallurgy and Materials in setting up the resonance facility is also gratefully acknowledged.

References

1. M. BRODT and R. S. LAKES, *Journal of Composite Materials* **29** (1995) 1823.
2. G. F. LEE, *Metallurgical and Materials Transactions A* **26A** (1995) 2819.
3. A. WOLFENDEN *et al., Journal of Materials Science* **30** (1995) 5502.
4. R. H. PANT and R. F. GIBSON, *J. Engineering Materials and Technology, Transactions of the ASME* **118** (1996) 554.
5. E. J. LAVERNIA *et al., Metallurgical and Materials Transactions A* **26A** (1995) 2803.
6. J. Y. LAI and K. F. YOUNG, *Composite Structures* **30** (1995) 25.
7. G. X. SUI *et al., Journal of Materials Science Letters* **14** (1995) 1218.
8. R. GREIF and B. HEBERT, *Journal of Engineering Materials and Technology* **117** (1995) 94.
9. Y. NISHINO, K. TANAHASHI and S. ASANO S, *Philosophical Magazine A* **71** (1995) 139.
10. P. C. WANG and R. J. FRIDRICH, *Journal of Composite Materials* **30** (1996) 1628.
11. I. JIMENO-FERNANDEZ *et al., Journal of Acoustical Society of America* **91** (1992) 2030.
12. S. S. KUMAR and P. R. MANTEMA, *Journal of Composite Materials* **30** (1996) 918.
13. R. LEETHAM and S. N. KUKUREKA, *Journal de Physique IV* **3** (1993) 1665.
14. S. SPINNER and W. E. TEFFT, *ASTM proceedings* **61** (1961) 1221.
15. G. PICKETT, *ibid.* **45** (1945) 846.
16. E. GOENS, *E. Annalen der Physik* **11** (1931) 649.
17. P. SACHS, in "Wind Forces in Engineering," 2nd ed. (Pergamon Press, 1978) 271.
18. C. A. HARPER, in "Handbook of Plastics, Elastomers, and Composites," 2nd ed. (McGraw-Hill, New York, 1992).
19. C. WEI, PhD Dissertation, The University of Birmingham, 1999.

Received 9 August
and accepted 10 December 1999